



**HAL**  
open science

## **Climate impact of stratospheric ozone recovery**

Slimane Bekki, Alexandru Rap, Virginie Poulain, Sandip Dhomse, Marion Marchand, Franck Lefèvre, Piers M. Forster, Sophie Laval-Szopa, Martyn P. Chipperfield

► **To cite this version:**

Slimane Bekki, Alexandru Rap, Virginie Poulain, Sandip Dhomse, Marion Marchand, et al.. Climate impact of stratospheric ozone recovery. *Geophysical Research Letters*, 2013, 40 (11), pp.2796-2800. 10.1002/grl.50358 . hal-00802252

**HAL Id: hal-00802252**

**<https://hal.science/hal-00802252>**

Submitted on 1 Apr 2016

**HAL** is a multi-disciplinary open access archive for the deposit and dissemination of scientific research documents, whether they are published or not. The documents may come from teaching and research institutions in France or abroad, or from public or private research centers.

L'archive ouverte pluridisciplinaire **HAL**, est destinée au dépôt et à la diffusion de documents scientifiques de niveau recherche, publiés ou non, émanant des établissements d'enseignement et de recherche français ou étrangers, des laboratoires publics ou privés.

## Climate impact of stratospheric ozone recovery

S. Bekki,<sup>1</sup> A. Rap,<sup>2</sup> V. Poulain,<sup>1</sup> S. Dhomse,<sup>2</sup> M. Marchand,<sup>1</sup> F. Lefevre,<sup>1</sup> P.M. Forster,<sup>2</sup>  
S. Szopa,<sup>3</sup> and M.P. Chipperfield<sup>2</sup>

Received 25 January 2013; revised 5 March 2013; accepted 11 March 2013; published 9 June 2013.

[1] Past stratospheric ozone depletion has acted to cool the Earth's surface. As the result of the phase-out of anthropogenic halogenated compounds emissions, stratospheric ozone is projected to recover and its radiative forcing (RF- $O_3 \sim -0.05 \text{ W/m}^2$  presently) might therefore be expected to decay in line with ozone recovery itself. Using results from chemistry-climate models, we find that, although model projections using a standard greenhouse gas scenario broadly agree on the future evolution of global ozone, they strongly disagree on RF- $O_3$  because of a large model spread in ozone changes in a narrow (several km thick) layer, in the northern lowermost stratosphere. Clearly, future changes in global stratospheric ozone cannot be considered an indicator of its overall RF. The multi-model mean RF- $O_3$  estimate for 2100 is  $+0.06 \text{ W/m}^2$  but with a range such that it could remain negative throughout this century or change sign and reach up to  $\sim -0.25 \text{ W/m}^2$ .

**Citation:** Bekki, S., A. Rap, V. Poulain, S. Dhomse, M. Marchand, F. Lefevre, P. M. Forster, S. Szopa, and M. P. Chipperfield (2013), Climate impact of stratospheric ozone recovery, *Geophys. Res. Lett.*, 40, 2796–2800, doi:10.1002/grl.50358.

### 1. Introduction

[2] Over the last 50 years, the atmospheric levels of chlorine and bromine species have been greatly enhanced by the anthropogenic release of compounds such as chlorofluorocarbons (CFCs) and halons. As a result, stratospheric ozone has decreased globally over the past few decades due to halogen-catalyzed chemical destruction. Following the Montreal Protocol and its amendments, the majority of CFC and halon emissions have been phased out and the atmospheric loading of these compounds is now decreasing from a peak at the end of the 20th century. Therefore, stratospheric ozone is projected to recover from the effects of anthropogenic chlorine and bromine-catalyzed destruction by the middle or end of the 21st century [Eyring *et al.*, 2010].

[3] Ozone is a radiatively important gas as it absorbs both short wavelength solar ultraviolet (UV) as well as thermal infrared (IR) radiation. Past stratospheric ozone depletion is estimated to have acted to cool the surface, i.e., it has a negative radiative forcing (RF). The latest estimates for RF of the stratospheric ozone depletion range between  $-0.03$

and  $-0.11 \text{ W/m}^2$  with a mean value of about  $-0.05 \text{ W/m}^2$  [Forster *et al.*, 2007; WMO, 2011; Cionni *et al.*, 2011; Hassler *et al.*, 2012], which has offset some of the warming from increased greenhouse gas (GHG) levels over the last few decades. Therefore, the future recovery of stratospheric ozone might naturally be expected to generate an RF of the opposite sign (i.e., positive) to the actual negative forcing. In this paper, we use predictions of the recovery of the ozone layer from a collection of state-of-the-art chemistry-climate models (CCMs) to investigate the radiative impact of stratospheric ozone recovery.

### 2. Model Runs

[4] We investigate the RF of a future stratospheric ozone recovery using ozone projections that were made by a range of CCMs (CCSRNIES, CMAM, GEOSCCM, LMDz-REPRO, MRI, SOCOL, ULAQ, UMSLIMCAT, and WACCM) within the framework of the SPARC (Stratospheric Processes and their Role in Climate) CCMVal-2 (Chemistry-Climate Model Validation phase 2) program [SPARC CCMVal, 2010]. Regarding the past, these nine CCMs are generally able to reproduce most of the structures of the ozone trends observed in the last three decades. For ozone projections, the evolution of GHGs in CCMs is forced according to the SRES A1B scenario which is close to the medium Representative Concentration Pathways (RCP) 6.0 scenario [Morgensten *et al.*, 2010], whereas the evolution of ozone-depleting substances (ODS) is forced according to the scenario A1 which is slightly modified to account for an earlier phase-out of hydrochlorofluorocarbons. Since ODS emissions are successfully controlled by the Montreal Protocol, the future evolution of ODS levels is much more certain than the evolution of GHG levels. The spread in CCM ozone projections originates from differences in present-day ozone calculations and in future model ozone trends [SPARC CCMVal, 2010; WMO, 2011]. Since the present-day ozone climatology is well known, the only actual uncertainty for future ozone is the ozone trend during the 21st century. In order to consider only the uncertainty in the ozone trend in the analysis, and not model biases in present-day ozone climatologies, 2100 ozone projections from individual models were reconstructed from a 2000 reference ozone climatology, taken as the 2000 multi-model mean (MMM) climatology, and from the global distribution of the 2000–2100 ozone trend from individual models. Before reconstruction, individual model projections are zonally averaged and smoothed with an 11-year running mean. As expected, the range of reconstructed ozone projections considered here is smaller than the actual range of CCMVal ozone projections [SPARC CCMVal, 2010]. The multi-model mean ozone projection (called MMMO<sub>3</sub> hereafter) represents simply the mean of individual model ozone projections and also corresponds to the ozone projection reconstructed

<sup>1</sup>LATMOS-IPSL, Paris, France.

<sup>2</sup>Institute for Climate and Atmospheric Science, School of Earth and Environment, University of Leeds, Leeds, UK.

<sup>3</sup>LSCE-IPSL, Saclay, France.

Corresponding author: S. Bekki, LATMOS-IPSL, Paris, France. (slimane.bekki@latmos.ipsl.fr)

from the zonal mean distribution of the MMM local ozone trend. The effect of ozone projection uncertainties on RF is evaluated by considering the ensemble of RFs calculated for individual model ozone projections. To identify the regions driving RF, we also consider the case of the MMM ozone projection (MMMO<sub>3</sub>) with lower stratospheric (LS) ozone remaining unchanged below 20 hPa during the 21st century (called MMMO<sub>3</sub>-US) and another case where middle and upper stratospheric (US) ozone remain unchanged above 20 hPa (called MMMO<sub>3</sub>-LS).

### 3. Results

#### 3.1. Ozone Changes

[5] Figure 1a shows the predicted evolution of global mean column O<sub>3</sub> from 1960 through 2100 under the standard A1B scenario for the MMMO<sub>3</sub> projection and for the range of individual model ozone projections. Individual model ozone projections were zonally averaged and smoothed with an 11-year running mean. Atmospheric measurements and model simulations constrained by emission inventories indicate that the increase in anthropogenic ODS (mostly CFCs) emissions was very marginal before 1960 [WMO, 2011]. Therefore, trends in stratospheric ozone are expected to be negligible before the 1960s compared to post-1960s changes. For the standard GHG A1B scenario, all the models predict a recovery of global stratospheric ozone during the 21st century. However, there are still significant differences in the timing and extent of ozone recovery between models. Global mean stratospheric ozone changes between 2000 and 2100 vary from 4.8 to 9.2% with an MMM of  $6.98 \pm 1.73\%$ , giving an inter-model range of 4.4% (~12 DU) (see Figure 1a and Table 1). Figure 1a also shows an example of projected evolutions from a CCM (LMDz-REPRO) under a variety of RCP GHG scenarios [Szopa et al., 2012] illustrating the effect of uncertainties in future GHGs emissions on ozone projections. The rate and extent of ozone recovery, as stratospheric chlorine and bromine loadings decrease towards their natural levels, is modified by the degree of GHG-induced climate change. Larger GHG loadings (higher RCPs) cause larger recovery due to stronger stratospheric cooling [Eyring et al., 2010]. For LMDz-REPRO projections, global mean stratospheric ozone changes between 2000 and the end of the century vary from about 5.8 to 8.6%, giving a single model range from GHG scenario uncertainties of 2.8% (~8 DU), which is approximately a factor 2 higher than the spread (~4 DU) calculated by the CAM3.5 CCM for the same RCP scenarios [Eyring et al., 2010]. These single model ranges from CCMs (LMDz-REPRO, CAM3.5) run under different possible GHG scenarios are smaller than the inter-model range (~12 DU) found for an ensemble CCMs run under the same single GHG scenario, suggesting that, in contrast to most important climate forcing agents, the dominant source of uncertainties in ozone projections is actually not future emissions but model uncertainties.

[6] More importantly with respect to RF, the recovery of stratospheric ozone is not at all spatially uniform. Figure 1b shows the column O<sub>3</sub> change between 2000 and 2100 as a function of latitude for individual model projections and the MMMO<sub>3</sub> projection. Column O<sub>3</sub> changes are weighted by  $\cos(\text{latitude})$  in order to identify directly changes that are the most relevant for global O<sub>3</sub>. Column O<sub>3</sub> increases at all latitudes except in the tropics for three models. The

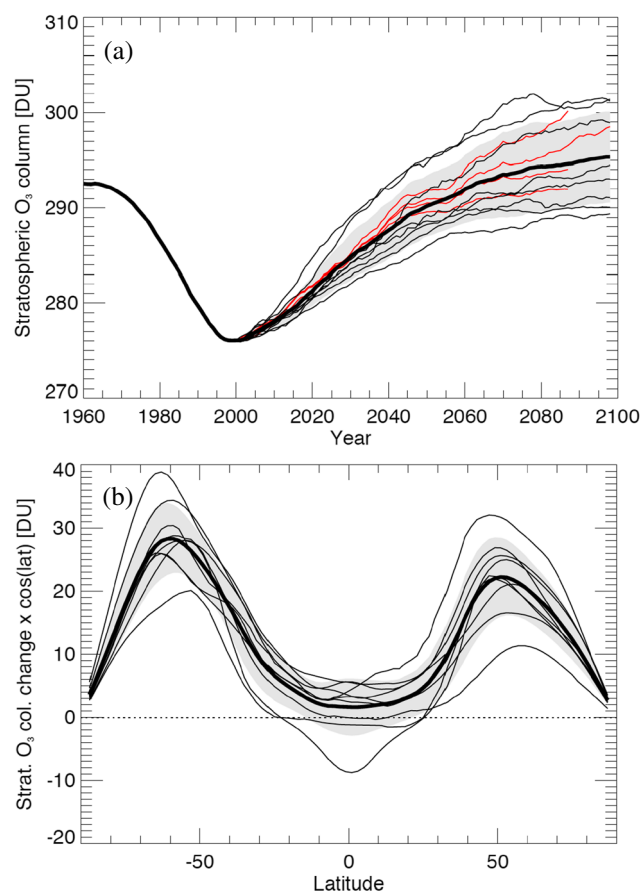


**Figure 1.** (a) Temporal evolution of the stratospheric globally averaged column ozone (DU) from 1960 to 2100 from individual CCMVal-2 model simulations forced according to the standard A1B scenario (thin black lines), from the MMM ozone projection (thick black line), and from LMDz-REPRO [Marchand et al., 2012] model simulations forced according to a range of RCP scenarios (thin red lines); the red lines correspond to (from bottom to top) RCP2.6, RCP4.5, A1B (close to RCP6.0), and RCP8.5 scenarios, respectively [taken from Szopa et al., 2012]. The gray shading indicates the  $1\sigma$  spread around the MMM globally averaged stratospheric column ozone. (b) Stratospheric column ozone change (DU) between 2100 and 2000 as a function of latitude from individual CCMVal-2 model simulations (thin black lines) and from the MMM stratospheric column ozone projection (thick black line). The gray shading indicates the  $1\sigma$  spread around the MMM latitude-dependent stratospheric column ozone change. Stratospheric column ozone changes in plot Figure 1b are weighted by  $\cos(\text{latitude})$ , which allows a comparison of the contributions of different latitude bands to the change in global mean stratospheric ozone.

most significant changes for global O<sub>3</sub> peak around 50–60° in both hemispheres. It is also where the model spread is the largest. The changes in tropical column ozone are much more modest in all the models. Figure 2a shows the annual zonal mean distribution of ozone changes between 2000 and 2100 in the MMMO<sub>3</sub> projection. Throughout most of the stratosphere, ozone increases over this period by up to 40%. The strongest ozone increases occur in the US and in the extra-tropical lowermost stratosphere (LMS) and tropopause region. Ozone decreases in the tropical LS reach up to 10%.

**Table 1.** Global Mean Stratospheric Ozone Change (%) and Radiative Forcing at the Tropopause ( $\text{W/m}^2$ ) for Different Scenarios of Ozone Changes in 2100 Relative to 2000<sup>a</sup>

Projection	Global Stratospheric Ozone Change (%)	Global Mean Radiative Forcing ( $\text{W/m}^2$ )
MMMO <sub>3</sub>	+6.98	+0.131
MMM ( $\sigma$ )	+6.98 ( $\pm 1.73$ )	+0.114 ( $\pm 0.079$ )
Model range	from +4.82 to +9.18	from $-0.001$ to +0.268
MMMO <sub>3</sub> -US (LS fixed)	+4.64	$-0.057$
MMMO <sub>3</sub> -LS (US fixed)	+2.34	+0.188

<sup>a</sup>The calculation of the stratospheric ozone column is based on a tropopause defined as the 100 ppbv O<sub>3</sub> contour [Prather et al., 2011]. The MMO<sub>3</sub> projection corresponds to the multi-model mean (MMM) ozone projection (i.e., mean of individual model ozone projections) and its RF is calculated from this mean ozone projection. The MMM projection listed in this table corresponds to the same mean ozone projection but its RF is calculated as the MMM RF (i.e., mean of individual model RFs that are calculated from individual model ozone projections). The standard deviations on the MMM ozone projection and MMM RF are indicated. The ranges of global ozone change and RF for individual model projections are also given. The MMO<sub>3</sub>-US projection corresponds to the MMO<sub>3</sub> ozone projection but with LS ozone remaining unchanged below 20 hPa during the 21st century. The MMO<sub>3</sub>-LS projection corresponds to MMO<sub>3</sub> but with middle and US ozone remaining unchanged above 20 hPa.

This is due to a stronger upwelling related to the strengthening of the Brewer-Dobson circulation in the 2100 atmosphere [WMO, 2011]. Although the models agree on the qualitative aspects of ozone recovery (i.e., general increase throughout most of the stratosphere except in the tropical LS), there are

substantial quantitative differences between models in terms of magnitude and spatial extent of those features. Figure 2b shows the global distribution of the standard deviation ( $\sigma$ ) of the MMM ozone trend. The most pronounced differences between models are found in the LMS and tropopause region with  $\sigma$  exceeding 10% at almost all latitudes. In contrast, there is a reasonably good agreement among models throughout most of the stratosphere (i.e., the upper part of the LS, the middle, and upper stratosphere) with  $\sigma$  ranging from 1 to 5%.

[7] In order to picture how exactly the uncertainties in ozone trend translate into a spread in ozone change distribution, we plot in Figures 2c and 2d ozone changes for two projections that are reconstructed from the MMM local ozone trends reduced or increased by 1 $\sigma$  (i.e., 1 standard deviation of the MMM local trend). The difference between the two projections, called hereafter MMO<sub>3</sub> -  $\sigma$  and MMO<sub>3</sub> +  $\sigma$ , can be viewed as indicative of the model range in ozone changes in the extratropics but not in the tropics because ozone changes in US and in LS are partly anti-correlated there. Indeed, as ozone recovers in the tropical US, less ultraviolet (UV) radiation reaches the LS, resulting in a slower chemical ozone production and hence reduced levels of ozone in LS. Therefore, the stronger the US ozone recovery in a model, the weaker the tropical LS ozone depletion. This well-known compensating mechanism, the so-called the “self-healing” effect (Rosenfield and Schoeberl, 2005; Portmann and Solomon, 2007), is not significant in the extratropics where UV radiation levels are lower all year and

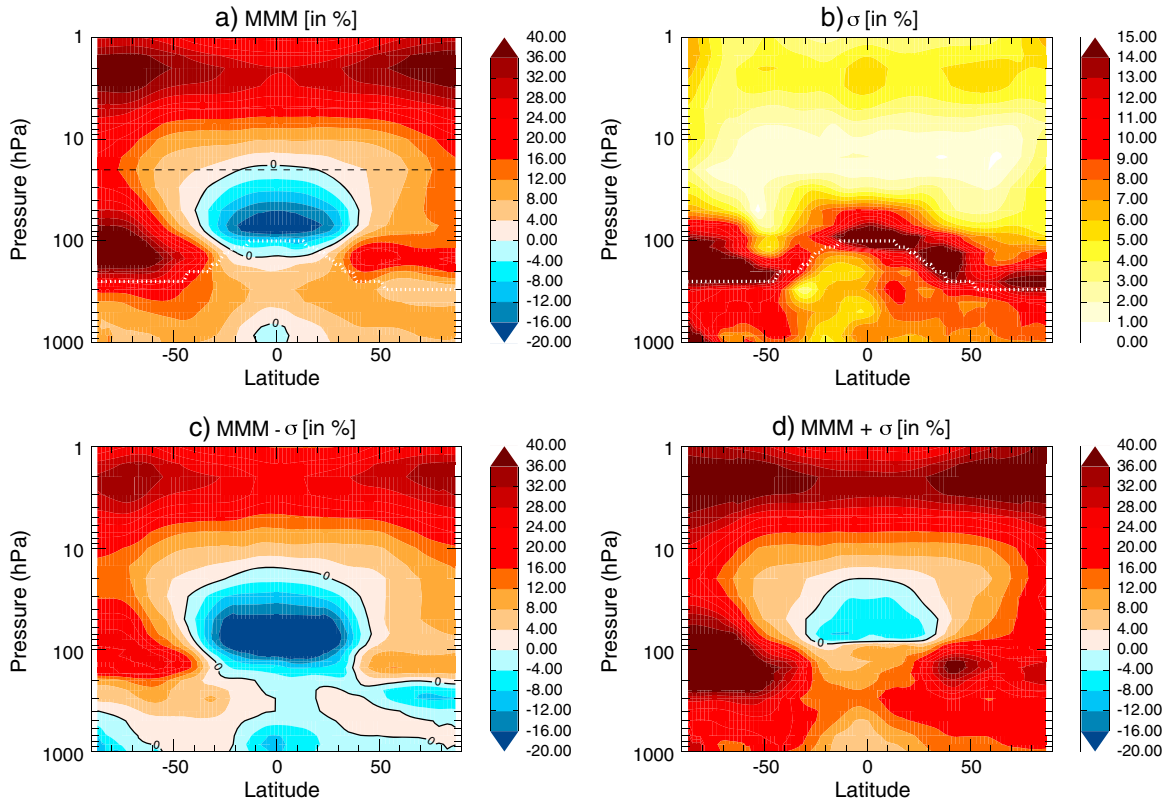


**Figure 2.** Difference in O<sub>3</sub> mixing ratio (%) between 2100 (A1B scenario) and 2000 from the CCMVal runs for (a) multi-model mean projection (MMMO<sub>3</sub>), (b) standard deviation on the MMO<sub>3</sub>, (c) MMO<sub>3</sub> -  $\sigma$  projection, and (d) MMO<sub>3</sub> +  $\sigma$  projection (see text for details). The black dashed horizontal line in Figure 2a indicates the 20 hPa level that represents the upper limit above which ozone remains unchanged in MMO<sub>3</sub>-LS and the lower limit below which ozone remains unchanged in MMO<sub>3</sub>-US. The white dotted lines in Figures 2a and 2b indicate the tropopause defined as the 100 ppbv O<sub>3</sub> contour [Prather et al., 2011].

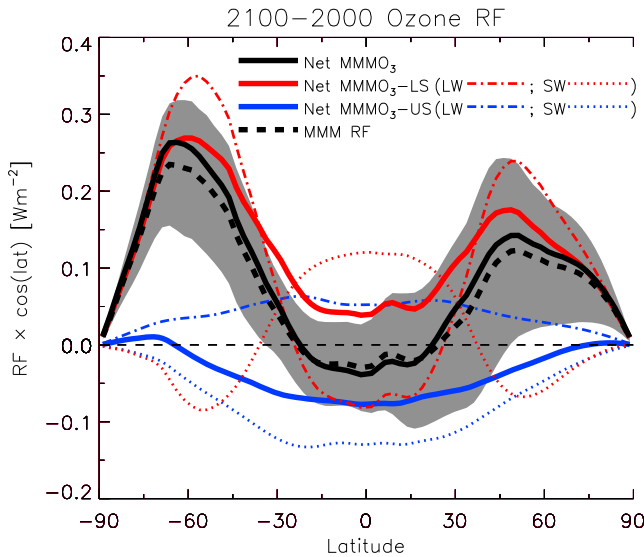


**Figure 3.** RF as a function of latitude. The RF values are weighted by  $\cos(\text{latitude})$ , which allows a comparison of the contributions of different latitude bands to the overall RF. The solid lines show RF from three projections:  $\text{MMMO}_3$  (black),  $\text{MMMO}_3\text{-LS}$  (US fixed) (red), and  $\text{MMMO}_3\text{-US}$  (LS fixed) (blue). The thick dashed line and the gray shading indicate the MMM RF and its  $\pm 1\sigma$  variations, respectively. Also shown are the LW and SW contributions to the total RF in the  $\text{MMMO}_3\text{-LS}$  and  $\text{MMMO}_3\text{-US}$  projections.

where the ozone budget is not dominated by upward transport and chemical production as in the tropics but by large-scale downward transport and chemical destruction. The largest difference between  $\text{MMMO}_3 - \sigma$  and  $\text{MMMO}_3 + \sigma$  projections is the sharp ozone enhancements in the extra-tropical LMS that are strongly attenuated in  $\text{MMMO}_3 - \sigma$  compared to  $\text{MMMO}_3 + \sigma$ ; for instance, the layer of ozone enhancement located between 100 and 200 hPa and extending poleward from  $20^\circ\text{N}$  is barely visible in the  $\text{MMMO}_3 - \sigma$  projection, and the extent of the LMS ozone increase at southern mid and high latitudes is also much smaller. In addition, the tropical LS ozone decline is vastly reduced below 50 hPa in  $\text{MMMO}_3 - \sigma$  compared to  $\text{MMMO}_3 + \sigma$ .

### 3.2. Radiative Forcing

[8] To estimate the stratospherically adjusted (using the fixed dynamic heating approximation) RF caused by the change in ozone from 2000 to 2100, we use the off-line version of the *Edwards and Slingo* [1996] radiation model. A climatology based on International Satellite Cloud Climatology Project clouds and European Center for Medium-Range Weather Forecasts reanalysis data for water vapor, temperature, and trace gas data was employed [for details, see *Rap et al.*, 2010]. Figure 3 shows the latitudinal variation of the MMM annual mean radiative forcing at the tropopause (expressed as  $\text{RF} \times \cos(\text{lat})$ ) derived from the ensemble of RFs calculated for individual model ozone projections; the standard deviation corresponds to the limits of the gray shading. The latitudinal variation of RF for the  $\text{MMMO}_3$ ,  $\text{MMMO}_3\text{-LS}$  and  $\text{MMMO}_3\text{-US}$  projections are also plotted in Figure 3. Table 1 provides the globally averaged values of RF for the different ozone projections. The MMM globally averaged RF (i.e. mean of the global RFs of individual model

ozone projections) is  $+0.11 \pm 0.08 \text{ W/m}^2$ . This value can be combined with the global RF of past stratospheric ozone depletion (about  $-0.05 \text{ W/m}^2$ ) to derive a best estimate of about  $+0.06 \text{ W/m}^2$  for the 2100 RF with respect to the pre-ozone depletion period (before the 1970s).

[9] As the latitudinal variation of RF and its global mean ( $+0.13 \text{ W/m}^2$ ) for the  $\text{MMMO}_3$  projection are very close to the latitudinal variation and global mean of the MMM RF (see Figure 3), we simply diagnose the different components of the radiative perturbations in the  $\text{MMMO}_3$  projection. The overall 2100 RF with respect to 2000 is dominated by the strongly positive RF at mid and high latitudes in both hemispheres (thick black line in Figure 3). According to the sensitivity simulations (red and blue lines in Figure 3), this positive RF in the extratropics is mostly due to the extensive ozone increases in the lower stratosphere below 20 hPa, which leads to a strong longwave (LW) warming. RF is slightly negative in the tropics where the negative shortwave (SW) RF caused by the US ozone increase, combined with the negative LW RF caused by the LS ozone decrease, outweighs the positive LW RF caused by the US ozone increase and the positive SW RF caused by the LS ozone decrease.

[10] While models agree relatively well on ozone changes in middle and upper stratosphere, the dispersion in ozone projections is considerable in the LMS and tropopause region resulting in large inter-model differences in the latitudinal variation of RF and in global RF. Individual model global mean RF ranges from  $-0.001$  to  $+0.268 \text{ W/m}^2$  with an MMM global RF of  $+0.11 \pm 0.079 \text{ W/m}^2$ . The correlation between global ozone changes and global RF is poor ( $r=0.38$ ). For instance, the individual model projection corresponding to the lowest global ozone change (4.82%) generates an RF ( $+0.14 \text{ W/m}^2$ ) greater than the MMM RF ( $+0.11 \text{ W/m}^2$ ), whereas the individual model projection generating the lowest global RF ( $-0.001 \text{ W/m}^2$ ) corresponds to a global ozone change (6.15%) quite close to the MMM global ozone change ( $\sim 7\%$ ). This illustrates how decoupled global ozone change and RF can be in model projections. Clearly, unlike most climate forcing agents (Forster *et al.*, 2007), the changes in global stratospheric ozone burden should not be considered a reliable indicator of its overall RF in the future.

[11] When considering a  $+1\sigma$  deviation in the MMM latitude-dependent RF (top limit of the gray shading in Figure 3), RF is found to be positive at all latitudes, whereas it becomes negative from  $40^\circ\text{S}$  to  $50^\circ\text{N}$  for a  $-1\sigma$  deviation (bottom limit of the gray shading in Figure 3). The spread in RF is most significant at northern mid-latitudes with a peak around  $40\text{--}50^\circ\text{N}$  (maximum in the width of the gray shading in Figure 3) and is caused by ozone enhancements between 100 and 200 hPa from about  $20^\circ\text{N}$  to  $60^\circ\text{N}$  that vary substantially from one model to another. Ozone enhancements in this region are strong and prominent in some individual model runs (see the  $\text{MMMO}_3 + \sigma$  ozone projection in Figure 2d), whereas they are relatively weak in other individual model runs (see the  $\text{MMMO}_3 - \sigma$  ozone projection in Figure 2c). Although smaller, the spread in RF is also substantial at southern mid and high latitudes. In the tropics, although the extent of the LS ozone decrease is severely reduced below 50 hPa in  $\text{MMMO}_3 - \sigma$  compared to  $\text{MMMO}_3 + \sigma$ , the spread in RF is relatively modest. This is due to the fact that tropical RF is most sensitive to ozone

changes in the altitude range between 10 and 40 hPa [Riese *et al.*, 2012] where the model spread is small (see Figure 2b). Note that, since RF calculations are performed with only one radiative transfer model, the range of stratospheric ozone RF presented here does not account for another source of model uncertainties, the radiative transfer modeling [Forster *et al.*, 2011]. However, it is unclear that different radiative transfer models applied on the same range of ozone projections would calculate very different spreads in RF, mostly because the differences between radiative models might be expected to be biases rather than random errors.

#### 4. Conclusions

[12] Although stratospheric ozone and its radiative forcing are thought to have evolved together in the last century, we show here that it is uncertain that the actual negative RF will now decay and disappear in line with the recovery of stratospheric ozone. According to our model-based analysis, the RF over the 2000–2100 horizon could either end up being negligible or exceed  $+0.25 \text{ W/m}^2$  making it comparable to the present-day tropospheric ozone forcing ( $\sim +0.35 \text{ W/m}^2$ , [Forster *et al.*, 2007]). In other words, stratospheric ozone might continue offsetting some of the positive GHG forcing during this century or become a significant contributor to global warming. The range of future stratospheric ozone RF would be even wider if the spectrum of model ozone projections accounted for uncertainties in future GHG emissions [see Figure 1; Eyring *et al.*, 2010; Szopa *et al.*, 2012]. It is worth pointing out that the possible change of sign in the climate forcing of stratospheric ozone and the fact that its global burden may not be an indicator of its overall climate forcing in the future are very unusual, if not unique, features among climate forcing agents [Forster *et al.*, 2007].

[13] The large spread in future RF of stratospheric ozone for a single GHG scenario originates from the wide range of ozone projections in the LMS and tropopause region, particularly at the northern mid latitudes. The ozone budget in this region is complex and several relevant processes such as in situ destruction, exchanges with the tropical and polar regions, and stratosphere/troposphere exchanges are likely not to be well simulated in global chemistry-climate models, partly because of their very coarse resolutions. Stratospheric ozone models have been designed to simulate the evolution of total column ozone in a changing environment and climate [SPARC CCMVal, 2010], mostly because total column ozone is the key stratospheric parameter regulating the amount of ultraviolet radiation reaching the Earth's surface, the primary concern of the Montreal protocol. As LMS ozone does not represent an important component of the total column, historically, it has not been the focus in stratospheric ozone chemistry-transport and chemistry-climate modeling. If the magnitude, or at least the sign, of future stratospheric ozone climate forcing is to be reliably predicted, the representation

of ozone processes in the lowermost stratosphere and tropopause region would need to be greatly improved in chemistry-climate models.

[14] **Acknowledgments.** We acknowledge the modeling groups for making their simulations available for this analysis, the Chemistry-Climate Model Validation (CCMVal) Activity for WCRP's (World Climate Research Programme), SPARC (Stratospheric Processes and their Role in Climate) project for organizing and coordinating the model data analysis activity, and the British Atmospheric Data Centre (BADC) for collecting and archiving the CCMVal model outputs. We also acknowledge the support of the RECONCILE EU project (funded by the European Commission under the grant number RECONCILE-226365-FP7-ENV-2008-1) and the U.K. Natural Environment Research Council. PMF acknowledges support from a Royal Society Wolfson Merit award.

#### References

- Cionni, I., et al. (2011), Ozone database in support of CMIP5 simulations: Results and corresponding radiative forcing, *Atmos. Chem. Phys.*, *11* (21), 11,267–11,292.
- Edwards, J. M., and A. Slingo (1996), Studies with a flexible new radiation code: I. Choosing a configuration for a large scale model, *Q. J. Roy. Meteorol. Soc.*, *122*, 689–720, doi:10.1002/qj.49712253107.
- Eyring, V., et al. (2010), Sensitivity of 21st century stratospheric ozone to greenhouse gas scenarios, *Geophys. Res. Lett.*, *37*, L16807, doi:10.1029/2010gl044443.
- Forster, P. M., et al. (2007), Changes in atmospheric constituents and in radiative forcing. In: *Climate Change 2007: The Physical Science Basis. Contribution of Working Group I to the Fourth Assessment Report of the Intergovernmental Panel on Climate Change*, edited by Solomon, S., D. Qin, M. Manning, Z. Chen, M. Marquis, K. B. Averyt, M. Tignor and H. L. Miller, Cambridge University Press, Cambridge, United Kingdom and New York, NY, USA.
- Forster, P. M., et al. (2011), Evaluation of radiation scheme performance within chemistry climate models, *J. Geophys. Res.*, *116*, doi:10.1029/2010JD015361.
- Portmann, R. W., and S. Solomon (2007), Indirect radiative forcing of the ozone layer during the 21st century, *Geophys. Res. Lett.*, *34*, L02813, doi:10.1029/2006GL028252.
- Hassler, B., et al. (2012), Comparison of three vertically resolved ozone data bases: Climatology, trends and radiative forcings, *Atmos. Chem. Phys. Discuss.*, *12*, 26,561–26,605.
- Marchand, M., et al. (2012), Dynamical amplification of the stratospheric solar response simulated with the chemistry-climate model LMDz-Reprobus, *J. Atmos. Sol-Terr. Phys.*, *75–76*, 147–160.
- Morgenstern, O., et al. (2010), Review of the formulation of present-generation stratospheric chemistry-climate models and associated external forcings, *J. Geophys. Res.*, *115*, D00M02, doi:10.1029/2009JD013728.
- Prather, M. J., et al. (2011), An atmospheric chemist in search of the tropopause, *J. Geophys. Res.*, *116*, D04306, doi:10.1029/2010JD014939.
- Rap, A., et al. (2010), Parameterisation of contrails in the UK Met Office climate model, *J. Geophys. Res.*, *115*, D10205, doi:10.1029/2009JD012443.
- Riese, M., et al. (2012), Impact of uncertainties in atmospheric mixing on simulated UTLS composition and related radiative effects, *J. Geophys. Res.*, *117*, doi:10.1029/2012JD017751.
- Rosenfeld, J., and M. Schoeberl (2005), Recovery of the tropical lower stratospheric ozone layer, *Geophys. Res. Lett.*, *32*(21), doi:10.1029/2005GL023626.
- SPARC CCMVal, SPARC Report on the Evaluation of Chemistry-Climate Models, V. Eyring, T. G. Shepherd, and D. W. Waugh (Eds.) (2010), SPARC Report No. 5, WCRP-132, WMO/TD-No. 1526, <http://www.atmos.physics.utoronto.ca/SPARC>.
- Szopa, S., et al. (2012), Aerosol and ozone changes as forcing for climate evolution between 1850 and 2100, *Clim. Dyn.*, doi:10.1007/s00382-012-1408-y.
- WMO (World Meteorological Organization) (2011), Scientific Assessment of Ozone Depletion: 2010, 516 pp., Geneva, Switzerland.